ORIGINAL PAPER

Investigation of controlled salmeterol xinafoate and fluticasone propionate release from double molecular imprinted nanoparticles

Esra Feyzioğlu-Demir[1,2] · Sinan Akgöl[3,4]

Abstract

Salmeterol xinafoate (SAM) and fluticasone propionate (FLU) are one of the drug combinations used together in the treatment of lung diseases such as asthma and chronic obstructive pulmonary disease (COPD). The aim of this study is to investigate the usability of novel dual molecular imprinted nanoparticles (poly(2-hydroxyethyl methacrylate-N-methacryloyl-(L)-alanine-N-methacryloyl-(L)-histidine) [p(HEMA-MAAL-MAH)], abbr. DMIPNPs) as a controlled drug release systems. In this study, SAM and FLU drugs were chosen as model drugs because they are used in the treatment of these diseases. DMIPNPs were prepared by surfactant-free emulsion polymerization method and characterized by scanning electron microscopy (SEM) and fourier transform infrared spectrometer (FTIR). In *in vitro* drug release experiments, drug release conditions were optimized. SAM and FLU release from DMIPNPs experiments were also performed in the simulated lung fluid (SLF). The amount of released SAM and FLU were found as 4.79 and 5.68 mg/g in the SLF medium at the end of 48 h, respectively. The release kinetics of SAM and FLU from DMIPNPs were calculated in the SLF medium. The release of SAM and FLU was determined to be compatible with the Higuchi release models. According to these results, these DMIPNPs, dual-template molecular imprinted nanoparticles with dual monomers, are promising materials that can be used in the controlled release of two different drugs.

Extended author information available on the last page of the article

Springer

Graphical abstract
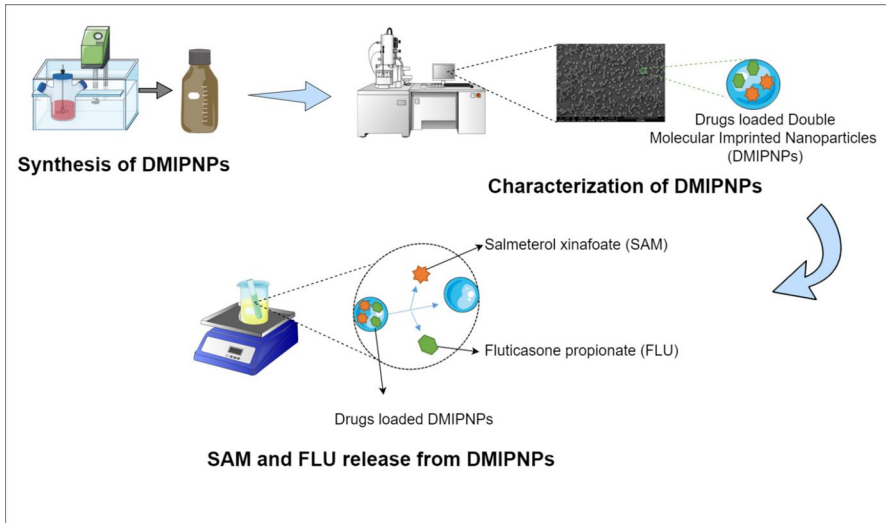
Introduction

The respiratory system is susceptible to many diseases such as asthma, bronchiolitis, chronic obstructive pulmonary disease (COPD), lung cancer, cystic fibrosis, and respiratory diseases in the newborn [1]. The most common of these diseases are asthma and COPD, also, their effects are gradually increasing. The number of asthma patients are increased by 5% every year. According to the report of World Health Organization (WHO), in the world, the number of asthma patients are 300 million, and it is estimated to increase to 400 million by 2025 [2]. COPD and asthma are characterized by obstruction of the airway. The obstruction in asthma is variable and reversible, while in COPD is persistent and largely irreversible. Both diseases have chronic inflammation due to an increase in the expression of very different inflammatory proteins in the respiratory tract [3, 4]. In the treatment of diseases such as asthma and COPD, the use of drugs by inhalation is often preferred because of its local and rapid effect. In particular, inhaled corticosteroids and β_2 adrenergic receptor agonists are frequently used in the treatment of asthma and COPD [5, 6]. Salmeterol xinafoate (SAM) is long-acting β_2-adrenoceptor agonist (LABA), while fluticasone propionate (FLU) is

in the inhaler corticosteroid (ICS), drug class. The SAM as a member of LABA induces bronchodilation and inhibition of the release of hypersensitivity mediators from mast cells. The FLU as a corticosteroid inhibits eosinophil activation and the subsequent release of inflammatory mediators. Combinations of SAM and FLU are often used to treat asthma and COPD because the combination of these drugs improves lung function and asthma symptoms more than using inhaled corticosteroids alone [7].

Pulmonary drug delivery is an alternative drug delivery system with many advantages over oral or injection delivery methods. Since lungs have a large surface area, thin alveolar epithelium, easily permeable membrane structure and a large vascular structure, they provide easy and fast absorption of soluble substances and drugs [8, 9]. In recent years, inhaled drug therapies have been successfully used in the treatment of topical asthma, local infectious diseases, local respiratory diseases such as pulmonary hypertension, cystic fibrosis, and some systemic diseases. Nanocarriers for pulmonary applications have been popular for the past two decades. The use of different nanocarriers such as polymeric nanoparticles, micelles, liposomes, dendrimers, mesoporous silica nanoparticles, and nanostructured lipid carriers are being invested for the pulmonary drug release [8]. Polymeric drug carriers cause to reduce the daily drug dose, and they provide drugs to diffuse easily due to particles size and surface properties. Nanoparticles also allow the retention of drugs to be prolonged by increasing their adhesion to the mucosal surface and reducing mucociliary clearance [10–12].

Molecular imprinted polymers (MIP) are relatively newer material than other carries materials using as drug delivery systems and use as drug delivery systems has been increasing in recent years [13]. MIPs have molecular recognition sites for the template (target) molecules, and they recognize template molecule specifically through binding sites. In addition, these specific binding sites allow binding template molecule with high selectivity and affinity. In the MIP synthesis, functional monomer and template molecule are formed precomplex by covalent bond or non-covalent interactions. At the end of the polymerization, the template molecule is removed from polymer to occur the specific binding sites for the target molecule. MIPs can be easy prepare with low cost. They have cross-linked polymeric nature and can be reused many times. In addition, MIPs have high stability and selective molecular recognition properties. For these reason, MIPs are the subject of intense many researches in the different applications [14–18]. In the drug release studies, molecular imprinted method increases the drug loading capacity and provides controlled drug release compared to conventional methods [13, 19]. MIPs are used as drug delivery carries in different routes such as transdermal, ocular, gastrointestinal, intravenous, stimuli-reactive routes, as it preserves its molecular recognition memory in different environmental conditions such as different temperatures, pH, and organic solvents [13, 17, 20]. In the literature, many different studies have been reported about MIP as a drug delivery carries. Cegłowski et al. [21] prepared molecularly imprinted polymers (MIPs) based on poly(2-isopropenyl-2-oxazoline) for 5-fluorouracil release. In the adsorption experiments, they determined the maximum adsorption 5-fluorouracil amounts. In addition, they calculated adsorption kinetics and adsorption isotherms parameters. In the vitro drug release experiments,

they investigated to 5-fluorouracil release in the different pH conditions. In the other study, Mohebali et al. [18] synthesized amitriptyline hydrochloride imprinted polymers (MIPS) and investigate to release of amitriptyline hydrochloride from these MIPs. In the another study, Raesian et al. [20] prepared and characterized fluorometholone molecular imprinted (MIP) lenses for using ocular controlled fluorometholone release.

Nowadays, different imprinting strategies such as surface imprinting, segment imprinting, and dual imprinting are improved for MIP in the different applications [22]. The one of these strategies is using multitemplate in other words dual template or multifunctional monomers in the synthesis of MIPs [23]. For example, Peng et al. [24] synthesized dual-template imprinting polymer nanoparticles (MIPs) with core–shell structure. In the synthesis, CD59 epitope protein and doxorubicin were used as dual template. They investigated the usability of these MIP nanoparticles in the cancer therapy. In the other study, Han et al. [25] prepared dual-template molecularly imprinted polymer (UIO-66@DMIPs) with using doxorubicin (DOX) and phycocyanin (PC) as template molecules. They investigate adsorption and release behavior of the drugs from UIO-66@DMIPs and cytotoxicity experiments were also carried out.

In this study, it is aimed to show the usability of previously synthesized double template molecular imprinted nanoparticles with dual monomers in controlled drug release. Since SAM and FLU are frequently preferred in the treatment of asthma and COPD, they were used as model drugs in this study. For this purpose, SAM and FLU imprinted DMIPNPS nanoparticles with dual monomers were prepared by surfactant-free emulsion polymerization methods. These DMIPNPs were characterized by FTIR and SEM. In the drug release studies, DMIPNPs whose drug loading capacities were determined in the previous study were used [23]. The release of SAM and FLU from DMIPNPs were also investigated with different release conditions such as pH, initial drug concentrations, and temperature. In the end of the release studies, SAM and FLU release studies were performed in SLF medium, and the release behavior of drugs was analyzed by using five different kinetic models including zero-order kinetics, first-order kinetics, Higuchi model and Hixson–Crowell models, and Korsmeyer–Peppas models.

Experimental section

Materials

Salmeterol xinafoate (SAM) and fluticasone propionate (FLU), hydroxyethyl methacrylate (HEMA), ethylene glycol dimethacrylate (EGDMA), potassium persulfate (KPS) and poly(vinyl alcohol) (PVA), methanol and other chemicals were purchased Sigma-Aldrich.

Synthesis of DMIPNPs

SAM and FLU imprinted DMIPNPs were synthesized by surfactant-free emulsion polymerization method as a mentioned in the previous study [23]. In this method, *N*-methacryloyl-(L)-alanine (MAAL) [26] and *N*-methacryloyl-(L)-histidine (MAH) [27] were used as functional monomers and synthesized as stated in the literature previously. Before the polymerization, SAM, template molecules, and MAAL, functional monomer, were mixed to prepare precomplex. At the same time, FLU, template molecules, and MAH, other functional monomer were also mixed in different vial bottles. The each of the precomplex solutions were stirred for 2 h. In the polymerization, PVA solution (stabilizer), HEMA monomer, EGDMA (crosslinker), precomplex solutions and KPS solution (initiator) were added to the reactor. This reactor was stirred at 70 °C for one hour in the shaking water bath after passing through nitrogen gas for 1–2 min to remove the oxygen. At the end of polymerization, DMIPNPs were washed several times with methanol and distilled water to remove unreacted substances. After the washing process, DMIPNPs were stirred in methanol/acetic acid (4:1) solutions for 4 days and in 1 M of NaCl/methanol (1:1) solution for 3 days with orbital stirring to remove SAM and FLU molecules from DMIPNPs. After this times, DMIPNPs were washed several times again with water to remove desorption agents. Finally, DMIPNPs were resuspended in water and stored at 4 °C until using in the experiments.

Non-imprinted nanoparticles (NIPNPs) were also prepared using the same methods without SAM and FLU molecules with using MAH, MAAL, and HEMA monomers. In addition, p(HEMA) nanoparticles containing only HEMA monomers were synthesized by the same method for characterization studies. A similar washing process was applied to these nanoparticles. In the synthesis of DMIPNPs, the potential interactions between drugs and monomers during the formation of precomplexes are shown in Fig. 1.

Characterization of DMIPNPs

The characterization of DMIPNPs were performed with attenuated total reflection-Fourier transform infrared spectrometer (ATR-FTIR), and scanning electron microscope (SEM). Detailed characterization of DMIPNPs has been mentioned in the previous study [23]. The functional groups of DMIPNPs were investigated by FTIR (ATR-PerkinElmer) using dried DMIPNPs in the oven. The surface morphology of DMIPNPs was analyzed by SEM (Quanta 250 S FEG). For this analysis, DMIPNPS nanoparticles were dried in an oven. Then, DMIPNPs were covered with gold for 2 min to increase conductivity of particles surfaces.

In vitro SAM and FLU loading and release studies

In the drug release studies, for drugs loading, the SAM and FLU drugs and DMIPNPS were mixed in methanol at a concentration of 1500 ppm SAM and FLU at 55 °C for 45 min. At the end of the time, DMIPNPs were centrifuged at
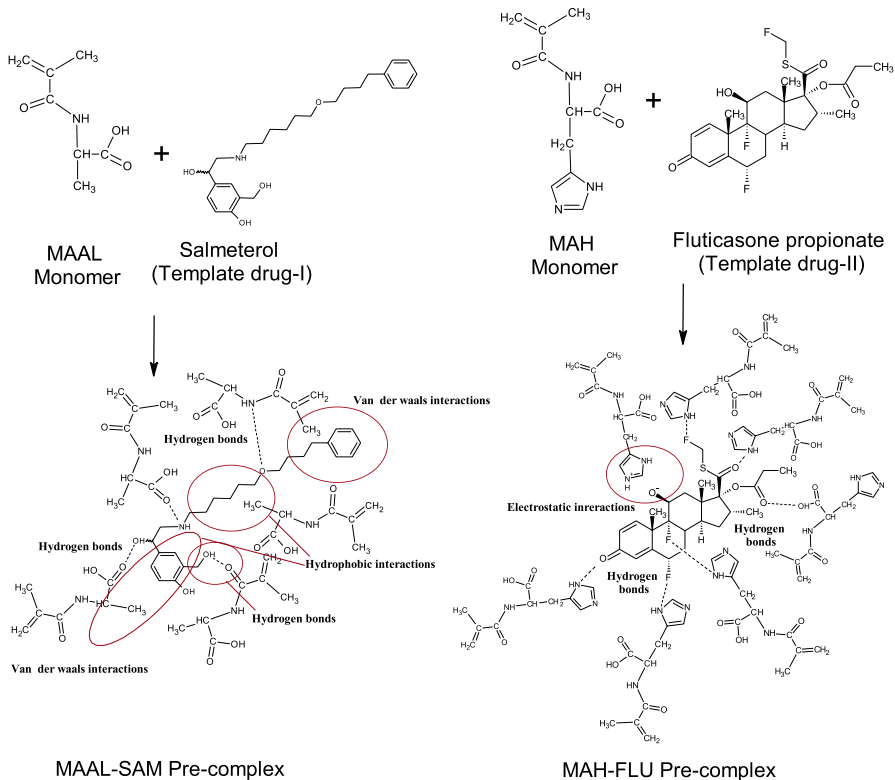
Fig. 1 Schematic illustration of potential interaction between drugs and monomers. This figure was created with ChemSketch application

14,500 rpm for 20 min, and the supernatant was analyzed by HPLC [28] to determine drug amounts. Shimadzu SCL-10AVP HPLC was used in the analysis with C18 column ODS-3 (4.6×150 mm, 5 μm of pore diameter; equipped with a guard column) as the stationary phase. Acetonitrile: 20 mM phosphate buffer pH 6.2 (70:30, %, *V:V*) was used as the mobile phase. Flow rate of mobile phase was set 1.5 mL/min, and temperature of column oven was also set to 30 °C. SAM and FLU drugs were analyzed at 228 nm wavelength. Before the HLP analysis, all samples were diluted with methanol 2 times and filtrated in the 0.45 μm porous membranes.

The amount of loaded SAM and FLU molecules on the DMIPNPs was calculated using the following equation [27, 29],

$$Q = \frac{\left(C_i - C_f\right) \times V}{m \times 10^{-3}} \tag{1}$$

where Q is the amount of SAM and FLU adsorbed on unit mass of the DMIPNPs (mg/g), C_i and C_f are initial and final concentration of SAM and FLU molecules (mg/L), respectively. V is the total volume of the solution (mL); and m is the dry
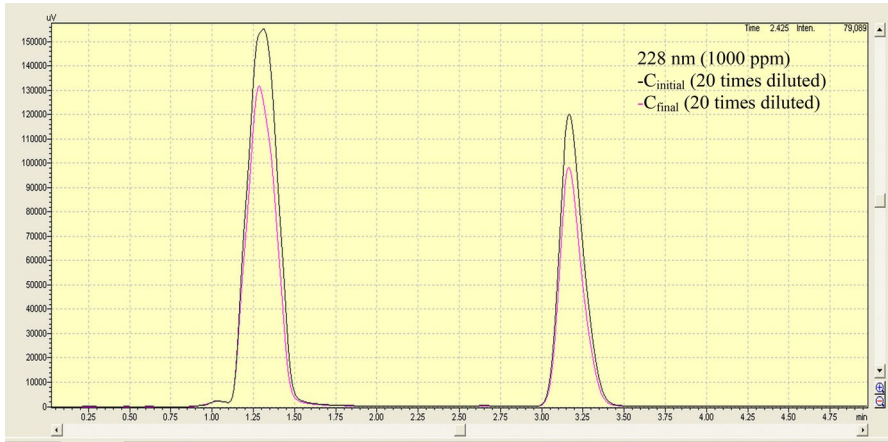
Fig. 2 Chromatogram of the initial and final concentrations of SAM and FLU solutions ($C_{initial} = 1000$ ppm SAM and FLU in the methanol at 37 °C; retention time of SAM and FLU = 1.35 min, 3.15 min, respectively

mass of DMIPNPs (mg). The chromatogram of initial and final concentration of SAM and FLU solutions obtained by this method is given in Fig. 2.

The release studies of SAM and FLU from DMIPNPs were carried out to investigate the effect of the pH, temperature, and initial drug concentration. In the pH studies, the experiments were performed in the different medium conditions in the range of pH 2.2 and pH 10.4. In order to effect of temperature on the SAM and FLU release, the experiments were practiced in the different temperature as 4, 25 and 37 °C. Choosing of these pH and temperature values were based on both chemical properties of drugs and monomers and physiological properties in the literature. Investigating the effect of loading drugs concentrations on the drugs release, the experiments were carried out with the 100, 500 and 1000 ppm drugs loading DMIPNPs. In these release studies, the loading SAM and FLU molecules on the DMIPNPs were carried out in the methanol for 45 min, at the 1000 ppm SAM and FLU solutions and in the 37 °C due to obtained maximum Q values from adsorption experiments.

In the drug release studies, dialysis membranes were used to separate DMIPNPs from the release medium. The 200 μL SAM and FLU loaded DMIPNPs was added into the dialysis membranes. These dialysis membranes were placed into 6 mL release medium and stirred in the water bath in 37 °C. After a certain time, samples were taken from the release medium and the same amount of fresh buffers were added into the release medium to keep the initial volume constant. The release of SAM and FLU from DMIPNPs were continued until reaching equilibrium in 48 h. Then, samples were measured using HPLC method as a mentioned above to determine amounts of SAM and FLU. The cumulative amounts of SAM and FLU (mg/g) were calculated against time.

The encapsulation efficiencies (EE) and loading capacities (LC) of DMIPNPs were also calculated using these following equations [30]:

$$\text{EE (\%)} = \frac{\text{(Total drug amounts} - \text{free drug amounts)}}{\text{Total drug amounts}} \times 100 \tag{2}$$

$$\text{LC (\%)} = \frac{\text{(Total drug amounts} - \text{free drug amounts)}}{\text{DMIPNPs weight}} \times 100 \tag{3}$$

In vitro SAM and FLU release from DMIPNPs in SLF medium

In the other part of release studies, simulated lung fluid (SLF) were prepared for investigated to *in vitro* SAM and FLU release behavior in the lung medium. Therefore, Gamble's solution which mimics the fluid environment deep in the lungs were prepared according to literature [31]. For this study, the optimum drug release conditions such as temperature, pH and initial drugs concentrations were chosen as 37 °C, pH 7.4 and 100 ppm, respectively. The SAM and FU release studies were performed as described above using Gamble's solution as a release medium. After taken samples, they were measured at 228 nm wavelength using HPLC method. Investigated of SAM and FLU release kinetics from DMIPNPs in SLF medium, five different kinetic models were used including zero-order kinetics, first-order kinetics, Higuchi model and Hixson–Crowell models, Korsmeyer–Peppas models. The equations of these release kinetic models are as follows:

$$\text{Zero-order kinetics}: \frac{M_t}{M_\infty} = k_d t \tag{4}$$

$$\text{First-order kinetics}: \log\left(100 - \frac{M_t}{M_\infty}\right) = \log 100 - k_1 t \tag{5}$$

$$\text{Higuchi model}: \frac{M_t}{M_\infty} = k_H \sqrt{t} \tag{6}$$

$$\text{Hixson-Crowell model}: \left(100 - \frac{M_t}{M_\infty}\right)^{\frac{1}{3}} = 100^{\frac{1}{3}} - k_{HC} t \tag{7}$$

$$\text{Korsmeyer-Peppas model}: \frac{M_t}{M_\infty} = k t^n \tag{8}$$

In these kinetics equations, the cumulative fractional drug release is shown in M_t/M_∞. The release time is stated by t. The zero-order rate constant, the first-order rate constant, the Higuchi rate constant, and the Hixson–Crowell rate constant are expressed by k_d, k_1, k_H, and k_{HC}, respectively. The kinetic constant for Korsmeyer–Peppas model and the diffusional exponent related to transport

mechanism Korsmeyer–Peppas model are stated by *k* and *n,* respectively. These equations are valid for the first 60% of the fractional release [32–35].

The Korsmeyer–Peppas model, also known as the power law, can be used to define the release behavior of Fickian diffusion, non-Fickian transport, and Case-II transport (zero-order (constant-rate)). The Korsmeyer–Peppas model equation can be also applied to different geometrical matrices such as spherical, cylinders, and thin film. For spherical geometries, when the value of *n* is 0.43, Fickian diffusion is defined. The non-Fickian transport, also known as anomalous transport, is described by $0.43 < n < 0.85$. The zero-order release (Case-II transport) is identified with the value of n is 0.85 [36].

Results and discussions

Synthesis and characterization of DMIPNPs

In the previous study, novel dual imprinted nanoparticles with dual functional monomers were prepared and characterized. Also their usability for adsorption of two drug molecules was demonstrated in detail [23]. In this study, DMIPNPs were synthesized in a similar way to investigate the usability of these DMIPNPs in controlled drugs release. For using in the FTIR analysis, p(HEMA-MAH) NPs and p(HEMA-MAAL) NPs were also prepared with same method as mention literature [27]. In the release experiments, nanoparticles whose drug adsorption conditions were determined in the previous study were used. Therefore, it could not optimize the drug loading conditions. The data obtained in this study were used. Because, SAM and FLU are often used treatment of respiratory disease such as asthma, these drugs are chosen as model drugs for novel developed imprinted nanoparticles. Schematically representation of usability of DMIPNPs in the treatment of asthma is shown in Fig. 3.

In the characterization studies, FTIR and SEM analysis were carried out. The FTIR spectrum of SAM and FLU imprinted DMIPNPs, NIPNPs, and p(HEMA) NPs is shown in Fig. 4. In the FTIR spectrums, O–H stretch vibration band (alcohol) is usually between 3300 and 3500 cm^{-1}. The spectrums of DMIPNPs, NIPNPs, and p(HEMA) NPs have O–H stretch vibration band around 3525.98, 3503.99, and 3444.95 cm^{-1}, respectively. The O–H stretch band of p(HEMA) NPs is sharper than the others spectra. Therefore, we can say that the hydroxyl groups of p(HEMA) NPs participate in bond formation. The alkane group of C–H stretch band is between 3000–2800 cm^{-1}. This C–H stretch bands of DMIPNPs, NIPNPs, and p(HEMA) NPs are shown at 2955.96, 2954.98, and 2952.94 cm^{-1}, respectively. In the all spectrums, the C=O (carbonly) stretch bands are founds around 1722 cm^{-1}. The spectrum of DMIPNPs has amine I bending band around 1637.97 cm^{-1} [23, 26, 27]. According to the SEM image in Fig. 5, DMIPNPs have almost spherical morphology. The particle size of DMIPNPs is about 269.6 ± 20.10 nm.
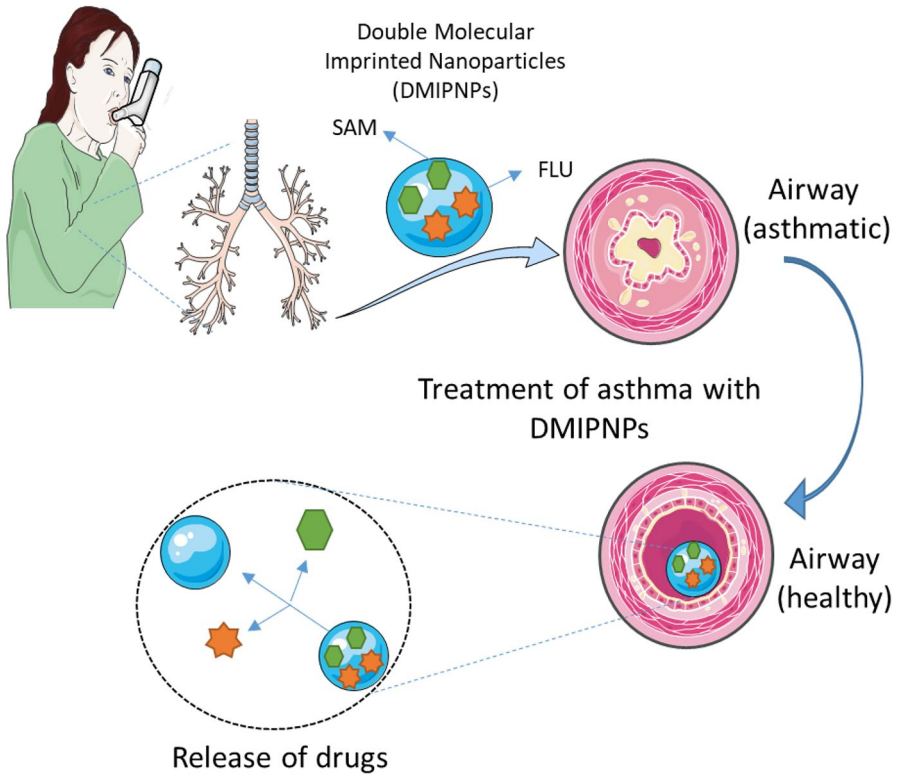
Fig. 3 Schematic representation of usability of DMIPNPs in the treatment of asthma. This figure was created using images from Servier medical art by Servier is licensed under a creative commons attribution 3.0 unported license, https://smart.servier.com

In vitro SAM and FLU loading and release studies

In the previous study, SAM and FLU adsorption conditions were investigated in drug adsorption studies and their adsorption came to equilibrium at a concentration of 1500 ppm SAM and FLU concentration in 45 min at 55 °C. The maximum SAM and FLU adsorption capacities of nanoparticles were found to be 537.64 and 393.32 mg/g, respectively, at 1500 ppm drugs concentration [23]. In drug release studies, the effect of the initial SAM and FLU concentrations, temperature and the pH was investigated to optimize the release conditions of SAM and FLU from DMIPNPs. The all release studies were performed in 48 h, and samples were taken at certain times.

The effect of initial drugs concentration

In the investigation of the effect of the initial SAM and FLU concentrations on the drug releases, releases studies were carried out with different drug loaded
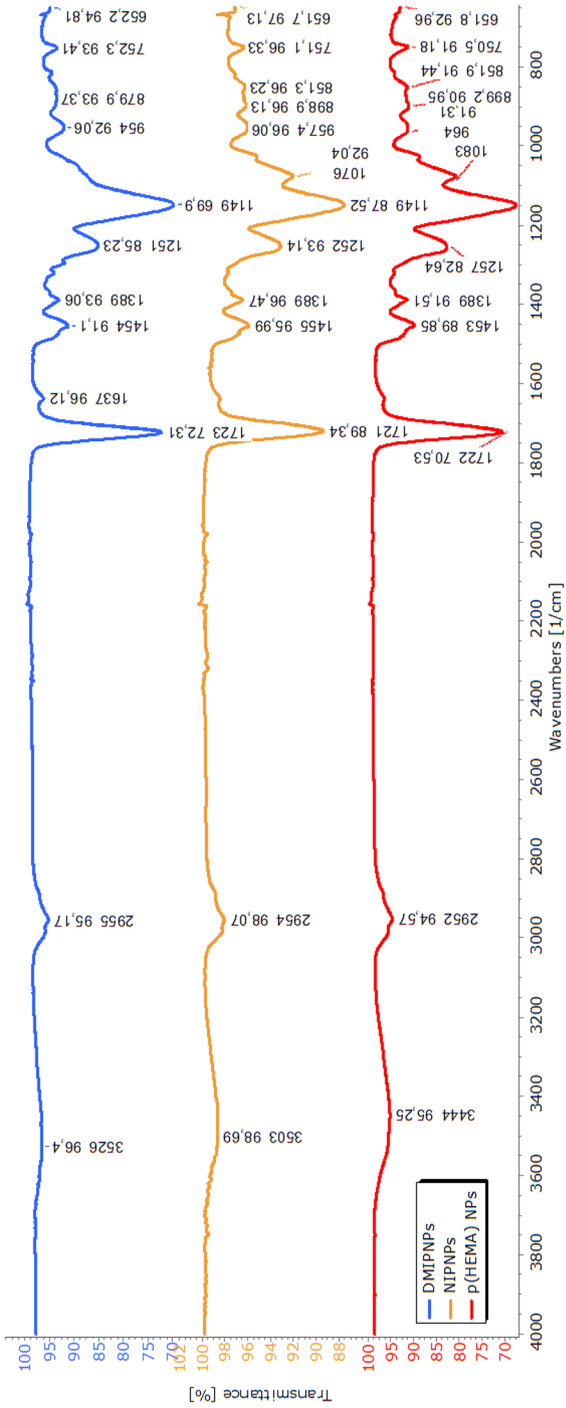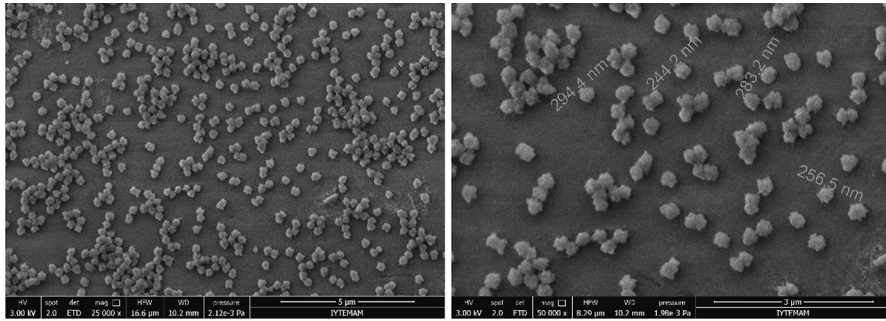
Fig. 4 ATR-FTIR spectrums of DMIPNPs, NIPNPs, and p(HEMA) NPs

Fig. 5 SEM photograph of DMIPNPs

Table 1 SAM and FLU encapsulation efficiencies and loading capacities of DMIPNPs

Drugs	Drug concentration (ppm)	Encapsulation efficiency (%)	Loading capacity (%)
SAM	100	12.95	4.34
SAM	500	20.74	8.60
SAM	1000	14.73	43.94
FLU	100	3.23	0.90
FLU	500	9.62	2.19
FLU	1000	14.07	33.43

DMIPNPs. For this purpose, SAM and FLU loading to DMIPNPs was performed by mixing 100, 500 and 1000 ppm SAM and FLU in methanol in a 37 °C water bath for 45 min. The encapsulation efficiencies (EE) and loading capacities (LC) of DMIPNPs are calculated and given Table 1. As seen Table 1, the encapsulation efficiencies of DMIPNPs to SAM and FLU were found to vary between 3.23% and 20.74% according to SAM and FLU concentrations. Similarly, the loading capacities of DMIPNPs to SAM and FLU were also found to vary between 0.90 and 43.94% according to SAM and FLU concentration. As given Fig. 6, when loaded SAM and FLU concentration were increased, the release amount of the SAM and FLU was also increased. At the end of 48 h, the maximum release of SAM and FLU amounts were determined as 19.30, 4.85 mg/g respectively, at 1000 ppm drugs concentrations.

The effect of pH

In the effect of pH on the SAM release studies, the maximum release was determined at pH 7.4 in phosphate buffer and the amount of the SAM was found as 20.34 mg/g at the end of the 48 h (in Fig. 7). In the synthesis of DMIPNPS nanoparticles, it is thought that hydrogen bonds, van der Waals interactions and hydrophobic interactions are dominated between SAM and MAAL monomers as seen Fig. 1.
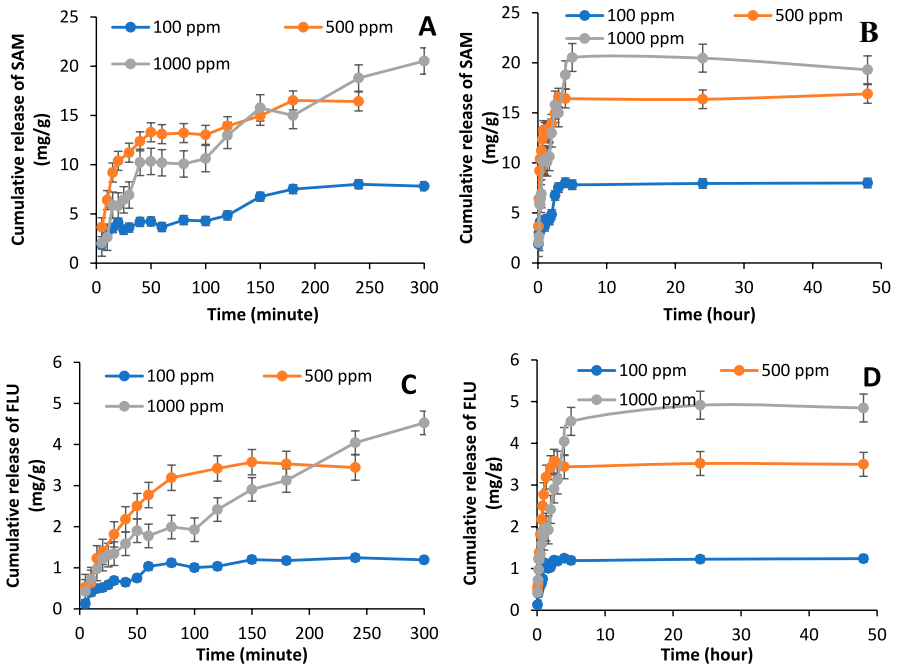
Fig. 6 Effect of the initial drug conditions on the SAM (**A** and **B**) and FLU (**C** and **D**) release from DIMPNPs (Time: 48 h, Temperature: 37 °C, in pH: 7.4 phosphate buffer)

Also because of the cavity on the nanoparticles in the synthesis of DMIPNPs which occur in the pH 6.4, this pH value is in the most suitable conformation for bonding to template. For this reason, it thought that the minimum release amount of the SAM was seen in the pH 6.4. Similarly, the maximum release of FLU was determined at pH 7.4 in phosphate buffer and the amount of the FLU was found as 4.85 mg/g at the end of the 48 h. In the synthesis of DMIPNPs, it is thought that electrostatic interactions and hydrogen bonds are dominated between FLU and MAH monomers as seen Fig. 1. The pKa value of imidazole in the histidine is approximately $pKa \approx 6$. Furthermore, three protonation states are observed between pH 1–14 corresponding to the imidazolium cation (at low pH), neutral imidazole-phenol ($pH \approx 5$–9), and the imidazole-phenolate anion (at high pH) [37]. For this reason, in pH 7.4, pH 6.4, and 8.2, the neutral imidazole is observed and the electrostatic interactions are decreased. Consequently, the FLU release is also increased. Because the cavity on the nanoparticles occurred at pH 6.4 in the synthesis of DMIPNPs, the binding cavity is the most suitable conformation for bonding to templates in this pH value. Therefore, the release amount of FLU was also decreased according to pH 7.4 and pH 8.2. In pH 2.2, the imidazole group is loaded with a positive charge, and the electrostatic interactions are increased. Therefore, the FLU release from DMIPNPs was also decreased. For this reason, the minimum FLU release was seen at a pH of 2.2.
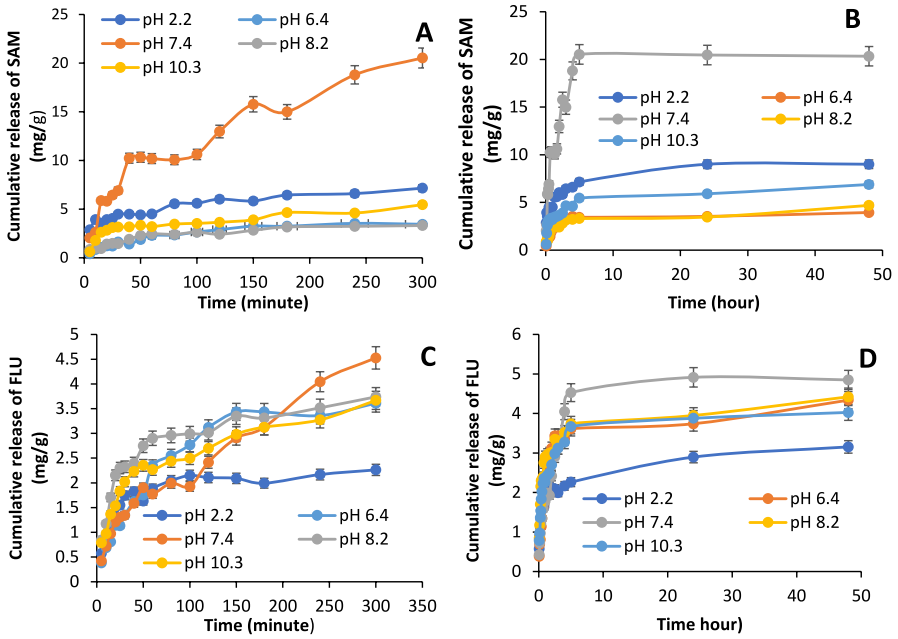
Fig. 7 Effect of the pH on the SAM (**A**, and **B**) and FLU (**C** and **D**) release from DIMPNPs ($C_{SAM \; and \; FLU \; initial}$: 1000 ppm, Time: 48 h, Temperature: 37 °C)
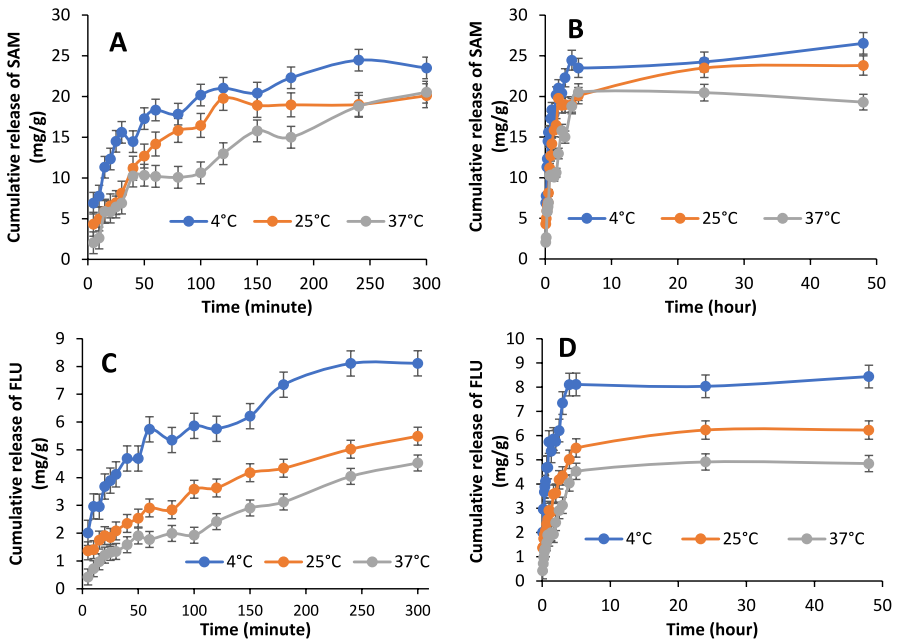
Fig. 8 Effect of the temperature on the SAM (**A** and **B**) and FLU (**C** and **D**) release from DIMPNPs ($C_{SAM \; and \; FLU \; initial}$: 1000 ppm, Time:48 h, in pH: 7.4 phosphate buffer)

The effect of temperature

In the effect of temperature on the SAM and FLU release studies, the maximum release amount of SAM and FLU were found as 26.53 and 8.44 mg/g at the end of the 48 h, respectively, as seen Fig. 8. The secondary interactions (hydrogen bonds, van der Waals interactions and hydrophobic interactions vb.) are dominated on the SAM and FLU adsorptions. When the temperature is increased, these interactions are also increased, and drug releases are decreased. Consequently, in accordance with adsorption studies, a decrease was observed in the amount of drug released as the temperature increased.

In Vitro SAM and FLU release from DMIPNPs in SLF medium

SLF medium was used to investigate the *in vitro* behavior of the release of SAM and FLU from DMIPNPs in the mimic lung environment. As given Fig. 9, the release amount of SAM and FLU were determined as 4.79, 5.68 mg/g at the end of 48 h, respectively, in the SLF medium. When the release amount of SAM compared with the release amount in 37 °C, pH 7.4 phosphate buffer, it appears to be lower in the SLF medium. Hydrogen bond, van der Waals and hydrophobic interactions are thought to be predominate between SAM and MAAL monomer. The pH value of SLF medium is 7.4 and contains lots of salts. As the amount of salt in the medium is increased, the hydrophobic interactions are also increased. Therefore, the amount of release is also decreased. For this reason, the lower amount
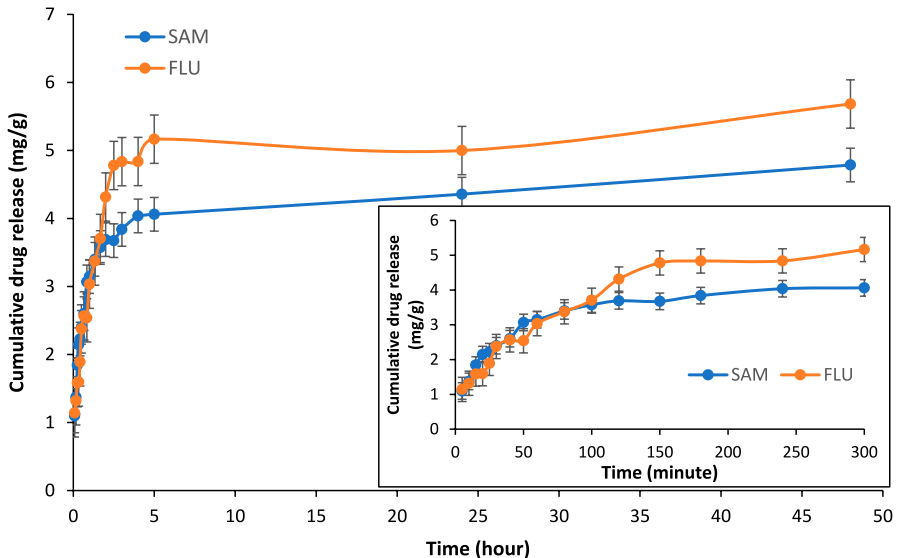

Fig. 9 SAM and FLU release from DIMPNPs in the simulated lung fluids (Drug loading: 1000 ppm in the methanol, 37 °C, 45 min; Release condition: in the SLF medium, 37 °C)

of SAM was obtained. While the amount of SAM released from DMIPNPs in the 5th hour is 82% of the total amount of SAM released, the amount of FLU is 84% of the total amount of FLU released. 50% of the release amount of SAM and FLU were found in 50th and 60th minutes respectively. Here, it is thought that be from the first burst effects. The first burst effect is due to drugs dispersed on the surface of the nanoparticles [38].

Release kinetics of SAM and FLU

Investigated to release kinetics of SAM and FLU from SAM and FLU imprinted DMIPNPs in the SLF medium, five different kinetic models were used to including zero-order kinetics, first-order kinetics, Higuchi model and Hixson–Crowell models, and Korsmeyer–Peppas models. The graphs of these kinetic models were plotted using the equations given above. These graphs are shown in Fig. 10.
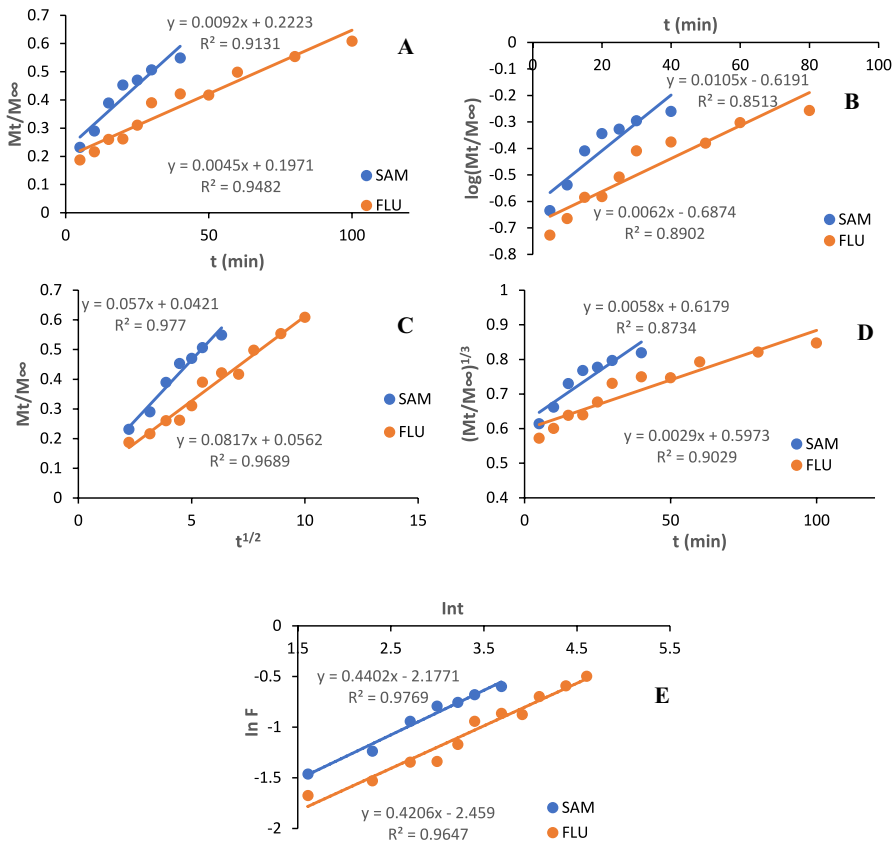
Fig. 10 Different kinetic release models of SAM and FLU. **A** Zero-order kinetic models, **B** First-order kinetic models, **C** Higuchi kinetic models, **D** Hixson–Crowell kinetic models and **E** Korsmeyer–Peppas kinetic models

Table 2 Drug release kinetic data obtained from SAM and FLU release experiments (n, diffusion exponent, k, kinetic constant; R^2, correlation coefficient)

	Zero-order kinetic		First-order kinetic		Higuchi model		Hixson–Crowell model		Korsmeyer–Peppas model		
	k_d	R^2	k_1	R^2	k	R^2	k_{HC}	R^2	n	k	R^2
SAM	0.009	0.9131	0.011	0.8513	0.057	0.977	0.006	0.8734	0.44	0.113	0.9769
FLU	0.005	0.9482	0.006	0.8902	0.0817	0.9689	0.003	0.9029	0.42	0.086	0.9647

The drug release kinetic data were calculated using the slope of these each graphs and given in Table 2. As seen Table 2, release kinetics models of SAM and FLU drugs were determined to be suitable with Higuchi model. According to the Higuchi model, the release of the drug from the matrix returns as the square root of a time-dependent process based on Fickian diffusion [33]. Peppas was used to diffusional exponent (n) for describe to drug transport mechanisms. According to SAM and FLU release from DMIPNPs results, it was determined that FLU release behavior from DMIPNPs was conformed to Fick diffusion model ($n = 0.42$), while SAM release behavior from DMIPNPs was also complied with non-Fickian transport model ($n = 0.44$). Fickian diffusional release occurs by the usual molecular diffusion of the drug due to its chemical potential [33].

In the literature, there are a few studies about encapsulated and released of SAM and FLU simultaneously. In the one study, fluticasone propionate and salmeterol xinafoate were microencapsulated in the modified chitosan microparticles [39]. In this study, trans-aconitic acid, succinic anhydride, 2-hydroxyethyl acrylate, and acrylic acid derived chitosan microparticles were prepared with particle size ranging from 0.4–22 μm. SAM and FLU loading capacities and encapsulation efficiency were calculated. It has been determined that SAM loading capacities vary between 2.1 and 11.18%, whereas FLU loading capacities are determined to change between 3.04 and 19.8%. The encapsulation efficiency of microparticles are also established to vary between 11.13 and 55.47%. In the drug release experiments, the release amount of SAM and FLU are found to be 25 and 9.5%, respectively, at the end of 100 h in the phosphate buffer adjusted at pH = 7.4. In the other study, fluticasone propionate and salmeterol xinafoate were nanoencapsulated by nanoaggregates using polyamides based on L-lysine [40]. These nanoaggregates were prepared by interfacial polycondensation method, and a nanocapsule with an average particle size of 226.7 ± 35.3 nm was obtained. The entrapment efficiency and encapsulated efficiency of nanoaggregates were calculated, and the entrapment efficiencies of nanoaggregates were found to change between 79.8 and 99.17%. The encapsulated efficiency of nanoaggregates were also determined to vary between 0.33 and 1.67%. The drug release studies were performed in phosphate buffer for 24 h. The release amount of SAM and FLU are found to be approximate 80 and 100%, respectively. At the end of study, five kinetic models such as zero-order kinetics, first-order kinetics, Higuchi model and Hixson–Crowell models,

and Korsmeyer–Peppas model parameters were calculated. It was found that the release profile of both FLU and SAM was suitable with the Higuchi model. Also, Korsmeyer–Peppas models were shown high correlation, and the value of n for FLU was found as 0.42 which indicated Fickian transport. The value of n for SAM was also determined as 0.44 which demonstrated non-Fickian diffusion.

Conclusions

In recent years, the use of molecular imprinted polymers as drug delivery systems has attracted attention. For this purpose, molecularly imprinted polymers with different forms and chemical structures are being developed. Although same dual/multi template imprinted polymers (MIPs) are reported in the literature, dual-template molecular imprinted nanoparticles with dual monomers are very few publications. For these reason, the usability of the previously synthesized novel dual-template molecular imprinted nanoparticles with dual monomers as drug delivery systems was investigated in this study. For this, the SAM and FLU drugs were used as dual templates. Because, these drug combinations are frequently used in the treatments of respiratory diseases such as asthma and COPD. In the drug release studies, the effect of drug release conditions such as initial drug concentration, pH and temperature on the drug release was investigated, and the maximum drug release was found at pH 7.4, in 1000 ppm, at 4 °C. Also, in the simulated lung fluid, the release amount of SAM and FLU were determined as 4.79, 5.68 mg/g at the end of 48 h, respectively. At the end of the study, drug release kinetics were calculated. The release behavior of SAM and FLU were found to be suitable with Higuchi model. While the diffusion of FLU from DMIPNPs occurred in accordance with Fickian diffusion modes, the diffusion of SAM was also occurred in accordance with non-Fickian transport. Considering all these results and compared with data in the literature, we can say that SAM and FLU imprinted DMIPNPs are hopeful novel dual-template molecular imprinted nanoparticles for drugs release.

Declaration

References

1. Smola M, Vandamme T, Sokolowski A (2008) Nanocarriers as pulmonary drug delivery systems to treat and to diagnose respiratory and nonrespiratory diseases. Int J Nanomedicine 3:1–19. https://doi.org/10.2147/IJN.S1045

2. Razavi-Termeh SV, Sadeghi-Niaraki A, Choi S-M (2021) Asthma-prone areas modeling using a machine learning model. Sci Rep 11:1912. https://doi.org/10.1038/s41598-021-81147-1

3. Barnes PJ (2008) Immunology of asthma and chronic obstructive pulmonary disease. Nat Rev Immunol 8:183–192. https://doi.org/10.1038/nri2254

4. Silva LFC, Kasten G, de Campos CEM et al (2013) Preparation and characterization of quercetin-loaded solid lipid microparticles for pulmonary delivery. Powder Technol 239:183–192. https://doi.org/10.1016/j.powtec.2013.01.037

5. Ali ME, McConville JT, Lamprecht A (2015) Pulmonary delivery of anti-inflammatory agents. Expert Opin Drug Deliv 12:929–945. https://doi.org/10.1517/17425247.2015.993968

6. Calzetta L, Ritondo BL, Matera MG et al (2020) Evaluation of fluticasone propionate/salmeterol for the treatment of COPD: a systematic review. Expert Rev Respir Med 14:621–635. https://doi.org/10.1080/17476348.2020.1743180

7. McKeage K, Keam SJ (2009) Salmeterol/fluticasone propionate. Drugs 69:1799–1828. https://doi.org/10.2165/11202210-000000000-00000

8. Garbuzenko OB, Mainelis G, Taratula O, Minko T (2014) Inhalation treatment of lung cancer: the influence of composition, size and shape of nanocarriers on their lung accumulation and retention. Cancer Biol Med 11:44–55. https://doi.org/10.7497/j.issn.2095-3941.2014.01.004

9. Oh YJ, Lee J, Seo JY et al (2011) Preparation of budesonide-loaded porous PLGA microparticles and their therapeutic efficacy in a murine asthma model. J Control Release 150:56–62. https://doi.org/10.1016/j.jconrel.2010.11.001

10. Beck-Broichsitter M, Merkel OM, Kissel T (2012) Controlled pulmonary drug and gene delivery using polymeric nano-carriers. J Control Release 161:214–224. https://doi.org/10.1016/j.jconrel.2011.12.004

11. Ungaro F, d'Angelo I, Miro A et al (2012) Engineered PLGA nano- and micro-carriers for pulmonary delivery: challenges and promises. J Pharm Pharmacol 64:1217–1235. https://doi.org/10.1111/j.2042-7158.2012.01486.x

12. Zhang J, Wu L, Chan HK, Watanabe W (2011) Formation, characterization, and fate of inhaled drug nanoparticles. Adv Drug Deliv Rev 63:441–455. https://doi.org/10.1016/j.addr.2010.11.002

13. Tang L, Zhao CY, Wang XH et al (2015) Macromolecular crowding of molecular imprinting: a facile pathway to produce drug delivery devices for zero-order sustained release. Int J Pharm 496:822–833. https://doi.org/10.1016/J.IJPHARM.2015.10.031

14. Büyüktiryaki S, Say R, Denizli A, Ersöz A (2007) Mimicking receptor for methylmercury preconcentration based on ion-imprinting. Talanta 71:699–705. https://doi.org/10.1016/j.talanta.2006.05.026

15. Ramström O, Ansell RJ (1998) Molecular imprinting technology: challenges and prospects for the future. Chirality 10:195–209. https://doi.org/10.1002/(SICI)1520-636X(1998)10:3%3c195::AID-CHIR1%3e3.0.CO;2-9

16. Han S, Song Y, Liu S et al (2022) Dual responsive molecularly imprinted polymers based on UiO-66-DOX for selective targeting tumor cells and controlled drug release. Eur Polym J 171:111219. https://doi.org/10.1016/J.EURPOLYMJ.2022.111219

17. He S, Zhang L, Bai S et al (2021) Advances of molecularly imprinted polymers (MIP) and the application in drug delivery. Eur Polym J 143:110179

18. Mohebali A, Abdouss M, Kazemi Y, Daneshnia S (2021) Fabrication and characterization of pH-responsive poly (methacrylic acid)-based molecularly imprinted polymers nanosphere for controlled release of amitriptyline hydrochloride. Polym Adv Technol 32:4386–4396. https://doi.org/10.1002/pat.5440

19. Hiratani H, Fujiwara A, Tamiya Y et al (2005) Ocular release of timolol from molecularly imprinted soft contact lenses. Biomaterials 26:1293–1298. https://doi.org/10.1016/j.biomaterials.2004.04.030

20. Raesian P, Rad MS, Khodaverdi E et al (2021) Preparation and characterization of fluorometholone molecular imprinted soft contact lenses as ocular controlled drug delivery systems. J Drug Deliv Sci Technol 64:102591. https://doi.org/10.1016/J.JDDST.2021.102591

21. Cegłowski M, Jerca VV, Jerca FA, Hoogenboom R (2020) Reduction-responsive molecularly imprinted poly (2-isopropenyl-2-oxazoline) for controlled release of anticancer agents. Pharmaceutics 12:506

22. Chen L, Wang X, Lu W, Wu X, Li J (2016) Molecular imprinting: perspectives and applications. Chem Soc Rev 45(8):2137–2211

23. Feyzioğlu Demir E, Akgöl S (2022) Synthesis and characterization of double molecular imprinted nanoparticles and investigation to adsorption of respiratory drugs. Polym Technol Mater 61:384–399. https://doi.org/10.1080/25740881.2021.1991949

24. Peng H, Qin Y-T, He X-W et al (2020) Epitope molecularly imprinted polymer nanoparticles for chemo-/photodynamic synergistic cancer therapy guided by targeted fluorescence imaging. ACS Appl Mater Interfaces 12:13360–13370. https://doi.org/10.1021/acsami.0c00468

25. Han S, Yao A, Ding Y et al (2022) A dual-template imprinted polymer based on amino-functionalized zirconium-based metal–organic framework for delivery of doxorubicin and phycocyanin with synergistic anticancer effect. Eur Polym J 170:111161. https://doi.org/10.1016/J.EURPOLYMJ.2022.111161

26. Garipcan B, Bereli N, Patır S et al (2001) Synthesis of poly[(hydroxyethyl methacrylate)-co-(methacrylamidoalanine)] membranes and their utilization as an affinity sorbent for lysozyme adsorption. Macromol Biosci 1:332–340

27. Uygun M, Feyzioğlu E, Özçalışkan E et al (2013) New generation ion-imprinted nanocarrier for removal of Cr (VI) from wastewater. J nanoparticle Res 15:1–11

28. Ammar HO, Ghorab MM, Mahmoud AA, Shahin HI (2017) Design and in vitro/in vivo evaluation of ultra-thin mucoadhesive buccal film containing fluticasone propionate. AAPS PharmSciTech. https://doi.org/10.1208/s12249-016-0496-0

29. Feyzioğlu Demir E, Öztürk Atay N, Koruyucu M et al (2018) Mannose based polymeric nanoparticles for lectin separation. Sep Sci Technol 53:2365–2375. https://doi.org/10.1080/01496395.2018.1452943

30. Sun L, Zhang X, Zheng C et al (2013) A pH gated glucose-sensitive nanoparticle based on worm-like mesoporous silica for controlled insulin release. J Phys Chem B. https://doi.org/10.1021/jp400442x

31. Marques MRC, Loebenberg R, Almukainzi M (2011) Simulated biological fluids with possible application in dissolution testing. Dissolution Technol 18:15–28. https://doi.org/10.1002/jps.23029

32. Arifin DY, Lee LY, Wang C-H (2006) Mathematical modeling and simulation of drug release from microspheres: implications to drug delivery systems. Adv Drug Deliv Rev 58:1274–1325. https://doi.org/10.1016/j.addr.2006.09.007

33. Guragain S, Torad NL, Alghamdi YG et al (2018) Synthesis of nanoporous calcium carbonate spheres using double hydrophilic block copolymer poly(acrylic acid-b-N-isopropylacrylamide). Mater Lett 230:143–147. https://doi.org/10.1016/J.MATLET.2018.07.060

34. Baglamis S, Feyzioğlu-Demir E, Akgöl S (2023) New insight into anti-wrinkle treatment: using nanoparticles as a controlled release system to increase acetyl octapeptide-3 efficiency. Polym Bull. https://doi.org/10.1007/s00289-022-04663-8

35. Korsmeyer RW, Peppas NA (1984) Solute and penetrant diffusion in swellable polymers. III. Drug release from glassy poly(HEMA-co-NVP) copolymers. J Control Release 1:89–98. https://doi.org/10.1016/0168-3659(84)90001-4

36. Siepmann J, Peppas NA (2012) Modeling of drug release from delivery systems based on hydroxypropyl methylcellulose (HPMC). Adv Drug Deliv Rev 64:163–174

37. Eseola AO, Obi-Egbedi NO (2010) Spectroscopic study of 2-, 4- and 5-substituents on pKa values of imidazole heterocycles prone to intramolecular proton-electrons transfer. Spectrochim Acta Part A Mol Biomol Spectrosc 75:693–701. https://doi.org/10.1016/j.saa.2009.11.041

38. Li H, Dong W, Zhou J et al (2013) Triggering effect of N-acetylglucosamine on retarded drug release from a lectin-anchored chitosan nanoparticles-in-microparticles system. Int J Pharm 449:37–43. https://doi.org/10.1016/j.ijpharm.2013.04.008

39. Ainali NM, Xanthopoulou E, Michailidou G, Zamboulis A, Bikiaris DN (2020) Microencapsulation of fluticasone propionate and salmeterol xinafoate in modified chitosan microparticles for release optimization. Molecules 25(17):3888. https://doi.org/10.3390/molecules25173888
40. Alyami MH, Dahmash EZ, Ali DK et al (2022) Novel fluticasone propionate and salmeterol fixed-dose combination nano-encapsulated particles using polyamide based on l-lysine. Pharmaceuticals. https://doi.org/10.3390/ph15030321

Authors and Affiliations

Esra Feyzioğlu-Demir[1,2] · **Sinan Akgöl[3,4]**

✉ Esra Feyzioğlu-Demir
esraa.feyzioglu@gmail.com

1 Department of Medical Laboratory Techniques, Vocational School of Health Services, Izmir University of Economics, 35330 Balçova, Izmir, Turkey

2 Department of Biotechnology, Graduate School of Natural and Applied Sciences, Ege University, 35100 Bornova, Izmir, Turkey

3 Department of Biochemistry, Faculty of Science, Ege University, 35100 Bornova, Izmir, Turkey

4 Sabanci University Nanotechnology Research and Application Center, 34956 Tuzla, Istanbul, Turkey